



Clark, D., Stevens, J. M., Tortonese, D., Whitehouse, M., Simpson, D., & Eldridge, J. (2019). Mapping the contact area of the patellofemoral joint: the relationship between stability and joint congruence. *Bone and Joint Journal*, 101-B(5), 552-558.
<https://doi.org/10.1302/0301-620X.101B5.BJJ-2018-1246.R1>

Peer reviewed version

Link to published version (if available):
[10.1302/0301-620X.101B5.BJJ-2018-1246.R1](https://doi.org/10.1302/0301-620X.101B5.BJJ-2018-1246.R1)

[Link to publication record in Explore Bristol Research](#)
PDF-document

This is the author accepted manuscript (AAM). The final published version (version of record) is BJS at <https://online.boneandjoint.org.uk/doi/full/10.1302/0301-620X.101B5.BJJ-2018-1246.R1> available online via . Please refer to any applicable terms of use of the publisher.

University of Bristol - Explore Bristol Research

General rights

This document is made available in accordance with publisher policies. Please cite only the published version using the reference above. Full terms of use are available:
<http://www.bristol.ac.uk/red/research-policy/pure/user-guides/ebr-terms/>

1 **Mapping the contact area of the patellofemoral joint: the**
2 **relationship between stability and congruence**

3
4 **AUTHORS:**

5 Damian Clark [1], Jarrad M Stevens [1], Domingo Tortonese [2], Michael R.
6 Whitehouse[1,3,4], Danielle Simpson [5], Jonathan Eldridge[1],

7
8 **INSTITUTION:**

9 1: Avon Orthopaedic Centre, Southmead Hospital Bristol, UK

10 2: Centre for applied anatomy, Univeristy of Bristol, UK

11 3: Musculoskeletal Research Unit, Translational Health Sciences, Bristol Medical
12 School, 1st Floor Learning & Research Building, Southmead Hospital, Bristol, BS10
13 5NB

14 4: National Institute for Health Research Bristol Biomedical Research Centre,
15 University Hospitals Bristol NHS Foundation Trust and University of Bristol

16 5: University of Nottingham Medical School

17
18 Damian Clark MBBS, FRCS, MSc

19 Jarrad Stevens, MBBS, ChM, FRACS, FAOrthA

20 Domingo Tortonese, D.V.M, PhD

21 Michael R Whitehouse PhD, MSc, BSc, MB ChB, FRCS(T&O), PG Cert(HE), FHEA

22 Danielle Simpson, BSc

23 Jonathan Eldridge, MBChB, BSc, FRCS, FRCS(T&O)

24
25 **CORRESPONDENCE:** drjarradstevens@hotmail.com

26 This study was supported by the NIHR Biomedical Research Centre at University
27 Hospitals Bristol NHS Foundation Trust and the University of Bristol. The views
28 expressed in this publication are those of the author(s) and not necessarily those of the
29 NHS, the National Institute for Health Research or the Department of Health and Social
30 Care.
31

Abstract:

Aims: (1) To determine and contrast the congruency through articular contact area of the patellofemoral joint during both active and passive movement of the knee with the use of an MRI control mapping technique. (2) Using the same method, to compare joint congruency for stable and unstable patellofemoral joints.

Method: A prospective case-control MRI imaging study of patients with a history of patellofemoral joint instability and volunteers with no knee symptoms was performed. The patellofemoral joints were imaged with the use of an MRI scan during both passive and active movement from 0 through to 40 degrees of flexion. The congruency through contact surface area was mapped in 5mm intervals on axial slices.

Results: Forty people took part in this study. The cases group included 31 patients who had symptomatic patellofemoral instability and the control group included nine asymptomatic volunteers. The unstable patellofemoral joints were demonstrably less congruent than the stable patellofemoral joints throughout the range of knee movement. The greatest mean differences between unstable and stable patellofemoral joint congruency were observed between 11 and 20 degrees flexion (1.73cm^2 vs 4.00cm^2 , $p<0.005$).

Conclusion: The congruency within the two groups for active and passive range of movement is closely correlated. The unstable patellofemoral joint is less congruent than the stable patellofemoral joint throughout knee movement. This approach to mapping

patellofemoral joint congruency may aid in the design of operations to increase stability and serve to assess pre- and post-operative interventions as a measurable outcome.

Introduction

The patellofemoral joint (PFJ) is geometrically complex, asymmetric and heavily influenced by kinematic forces about the knee. Patella engagement and subsequent congruence of the patella in the trochlear groove provides stability and dispersion of forces across the articulating surfaces with conformity of shape and movement.

In 1976, Goodfellow described changes in contact area that occur in the normal knee with the distal patella engaging in extension while the proximal patella articulated in flexion [1]. In the unstable joint, the patella will articulate in an abnormal manner to produce uneven distribution of forces presenting as subluxation and even dislocation of the patella. Incongruency of the patellofemoral joint, even without patella dislocation, leads to degenerative changes [2-7].

Visualising the congruency of the PFJ through imaging modalities is useful for establishing diagnosis, planning operative intervention and evaluating post-operative intervention [8]. Methods for assessing the PFJ include plain radiographs, ultrasound scan, computerised tomography (CT), magnetic resonance imaging (MRI) and three-dimensional computer navigation [8-12]. Accurate assessment of the congruency of the PFJ is vital in understanding the relationship of the bone and cartilage architecture, vectors about the joint and soft tissue restraints.

In order to improve objective MRI analysis of the unstable PFJ, we sought to map contact area through a range of passive and quadriceps active movement. Although this technique is not designed to be utilised as a routine investigation, we have

undertaken this study to document quantifiable measurements of the unstable PFJ. Additionally, we performed this imaging study on a control group of stable knees for a comparison and documentation of normal contact area throughout range of movement. Our hypothesis is that the unstable joint will be less congruent than the stable joint through passive and quadriceps active range of movement when mapped on multiple sequence MRI scan. With the ability to quantify congruency, the authors intend to compare pre- and post-stabilisation surgery contact area utilising this same technique. The clinical importance of this is demonstrated through the ability to objectively measure PFJ contact area and hence compare the pre-operative unstable joint with the change in contact area and perhaps the effectiveness of surgery with post-operative MRI mapping. With the aid of the results from this study, researchers will be able to compare surgical cases to a baseline cohort of patients with stable knees.

The aims of the study were: (1) To describe the articulating surface area of the PFJ in both active and passive movement; (2) To compare joint contact area using this method for stable and unstable patellofemoral joints.

Material and methods

This study has ethical approval (12/SW/0155) and all participants gave written informed consent. A single centre, prospective case-control MRI imaging study of patients with PFJ instability (cases n=31) and volunteers with no PFJ symptoms (controls n=9) was performed. An MRI scan was used to capture the PFJ articular cartilage contact area in a range of degrees of knee flexion in both quadriceps active and passive positions for both cohorts. MRI was selected as it permits assessment of anatomy in the axial, coronal and sagittal plan but can be oriented to any anatomical

axis which was needed for the dynamic assessment performed in this study. The advantage over CT is that it permits more accurate assessment of congruence by accounting for articular cartilage as well as bone. It is non-destructive and does not involve ionising radiation and is therefore suitable for cases and controls.

The cohort size was based on a two sample independent t-test with a mean difference of 2cm² with equal standard deviation of 1.75, power of 80%, and type I error =0.05 with a sampling ratio of 3:1 (cases:controls) yielding a minimum required sample size of 27 cases and nine controls. Our actual study size was 31 cases and nine controls.

Inclusion criteria for the cases cohort included patellofemoral joint instability for consideration of surgical management. The diagnosis of instability was a culmination of history (which included at least two prior episodes of patella dislocation), examination, and imaging investigations. Inclusion into the control group required volunteers who reported no symptoms currently or previously from the PFJ, and demonstrated normal knee examination with no clinical signs of instability.

The exclusion criteria included patients who were unable to provide valid consent, were unwilling to participate, aged 17 years or less, suffered degenerative knee joint disease (including any evidence of osteoarthritis observed on radiographs AP, lateral and skyline views), were pregnant, a history of metal objects or the possibility of metal object in soft tissues, particularly brain, eye, heart, spinal cord or if they were uncontactable by telephone.

The case subjects were recruited from the patient waiting list for surgery at a tertiary elective orthopaedic unit. Ninety-one consecutive patients were considered to be potentially eligible case subjects based on inclusion criteria. Of these, 72 were willing to discuss the study and 39 agreed to participate. There were eight patient withdrawals, leaving a cohort size of 31 (flowchart seen in Figure 1).

Information regarding; age, symptoms, previous dislocations, hypermobility and imaging results (Tibial Tuberosity Trochlear Groove, Insall Salvati Ratio, Biedert Patellotrochlear Index, Dejour grade) were obtained from patient notes and Picture Archiving and Communications Systems (PACS).

The control group was used to define normal values and validate the study methodology. Nine healthy volunteers were recruited from the hospital staff and researcher group who demonstrated normal knee and no history of patellofemoral joint symptoms. No formal imaging prior to the MRI scan was organised for participants in the control group.

Figure 1: Flowchart of patient inclusion and exclusion.

MRI Scanner:

MRI was performed with a GE Discovery MR450 1.5 tesla scanner and an eight-channel cardiac coil. The subject underwent a standard checklist where they were asked specific questions regarding comfort and safety in the MRI scanner.

Patient Position:

The subject lay supine on the MRI table with a triangular wedge under the knee and a strap over the thighs in order to maintain the position of the femur during the examination (Figure 2A). Data was captured in both passive and quadriceps active movement.

The initial localiser MRI sequence performed was an ultrafast gradient echo 3 plane localiser. The localiser scan permitted the technician to identify the boundaries of the

trochlea and plan the location of the definitive scan. The scan boundaries were placed beyond the boundaries of the trochlea in order to ensure full capture of the area of interest. Blocks of axial images were captured with one sagittal localiser to calculate the precise knee flexion position. The axial image was centred over the trochlea and then as the knee extended the patella came into view, maintaining at all times the same series of images of the trochlea.

Passive movement imaging:

The patient was secured as above and the knee permitted to rest at 40 degrees of flexion, a series of images was captured. A further foam cushion was placed under the heel to attain a scan at 20 degrees of flexion, finally a further cushion was placed to attain a scan at 0 degrees of flexion and the series repeated a further time (Figure 2B). The angle of flexion was recorded by means of tibiofemoral angle on the sagittal localiser image as opposed to the thigh-calf angle used to position the patient.

Quadriceps active imaging:

The patient was positioned supine with a triangular foam pillow under the knee. A beach ball was placed anterior to the tibia with a valve under the control of the subject (Figure 3). The subject was requested to extend the knee, pushing the lower leg against the balloon, causing it to deflate (Figure 2C). Subjects were advised that it would be expected to take two minutes to achieve this. The MRI operator informed the subject that the scan was due to start so as to coincide this with the beginning of the scan. As the knee extended the scan was begun and repeated whilst the subject deflated the balloon.

Rapid sequence axial images were captured whilst the ball was permitted to continue to deflate under the subject's control. The deflation rate was dependent upon the exertion of the patient and was not externally controlled. Five to eight sequences were captured per deflation.

Imaging sequence:

After the localiser scan located the distal femur, the sequence placement was planned so that the entire trochlea could be imaged. In both the active and passive modes, the thigh did not move due to control by strapping and it was possible to attain adequate quality imaging of the trochlea, without motion artefact. In each sequence, images captured included one sagittal slice and 10-18 axial slices (dependent on patient size) at 5mm intervals.

In any given scan, up to 5 images demonstrated contact between the patella and the trochlea and at any given moment, the entire trochlea was captured in order to ensure all the relevant images along the path of the patella were captured.

Image interpretation:

Using digital data supplied by the institutional PACS (GE Healthcare Centricity™ & Fujifilm Synapse™) the operator manually identified boundaries of cartilage contact between the patella and femur on both sides of the trochlear sulcus on the axial view. These measurements were recorded as linear distances. Each slice is 5mm wide and the surface area of each slice was calculated by multiplying the length by 5mm. Each slice surface is then summed to reach a measure of the surface area in contact between the

articulating surfaces to give a measure of congruency in each measurement condition. This was recorded on a “flattened” 2D coronal plane image for visual interpretation of contact area (Figure 4).

Statistical methods:

The repeatability of the measurements of MRI congruity were assessed by Pearson’s correlation coefficient. The measurements were repeated by the primary investigator at a second timepoint to give a measure of intra-observer error. The measurements were repeated by another observer for assessment of inter-observer error. Comparison between case and control variables was made with a Fisher’s exact test or Chi² test for categorical variables depending upon number of groups or independent t-tests for continuous data. Two-tailed independent sample t-tests were used to compare the mean joint congruence (cm²) between cases and controls during the different phases of knee flexion during quadriceps activation (0 degrees, 0-10, 11-20, 21-30, 31-40, >40 and combined). All statistical analyses were performed using SPSS (IBM SPSS Statistics, Armonk, NY, USA).

Results:

Between the cases and controls, the ages were well balanced. The mean age was 25 (range: 16-42; SD 6.9) in the case group and 26 (range: 19-32; SD 5.1) in the controls (p=0.690; Table 1). There were 19 females and 12 males in the cases group (p=0.060; Table 2). Laterality (side studied) was also well balanced, 36% being left amongst the cases and 44% amongst the controls (p=0.705). The other co-variates of interest that are associated with the pathology were more frequent amongst the cases than the

controls (Table 2). All patients in the cases group had sustained at least 2 dislocations with 19 (61%) sustaining more than 2 dislocations. Seven (22.6%) of the cases cohort have hypermobility with a Beighton score of four or more. Only six (19%) patients in the cases cohort demonstrated a normal trochlear groove with the 14 patients (45%) displaying Dejour C abnormalities. Unsurprisingly, all control group patients demonstrated a normal trochlear groove.

The radiological measurements were highly correlated for intra-observer error (0.985) and for inter-observer error (0.910). The congruency within the two groups for active and passive range of movement is closely correlated (Figure 5). The histogram illustrates the trend from incongruence to congruency as the knee flexes (Figure 6). The greatest differences in congruency between controls and cases is seen in the quadriceps active group between the range of zero and twenty degrees. The greatest mean differences and greatest statistical significance is at the 11-20 degree range (Figure 6). The curves match well between controls and cases; the exception is at the 40+ range where there only one case has been recorded and the trend for increased congruence is not observed.

Discussion:

The clinical importance of this study is to establish a direct measurement of PFJ contact area. With the ability to quantify congruency, the authors intend to use this technique to compare pre-operative and post-operative in cases where stabilisation surgery is performed.

With the aid of the results from this study, researchers will be able to compare surgical cases to a baseline cohort of patients with stable knees. The range 11-20

degrees (tibiofemoral angle) is the most sensitive. Clinicians may use the routine MRI performed in this position to evaluate congruence by this technique.

The PFJ is a complex articulation for which accurate assessment of congruence and morphology may remain elusive with a single imaging modality or if viewed in a single plane [13,14]. Our sequential MRI scans during active and passive range of movement of the knees demonstrated close correlation of contact area within the groups for both active and passive range of movement. When the control and cases groups are compared, the mean contact area was greater in the control group through all ranges of movement in both passive and quadriceps active with the exception of quadriceps active in extension. This may be secondary to an abnormal articulation of the unstable patella within the trochlear by activation of the quadriceps in this position.

The greatest mean differences between unstable and stable patellofemoral joint congruency during quadriceps active series were observed between 11 and 20 degrees (1.73cm^2 vs 4.00cm^2 , $p<0.001$). This is important as lateral patellar displacement has been shown to occur with the lowest restraining forces required at 20 degrees of knee flexion [15].

Understanding articular contact through imaging modalities is problematic with significant mismatch between osseous landmarks observed in radiographs or CT scans and the articular cartilage of the patella and trochlea obtained by an MRI [16]. Patella position has been evaluated with the use of many different indexes, such as the Insall-Salvati [17], the modified Insall-Salvati [18] the Blackburne-Peel [19], the Caton-Deschamps [20] and the Sagittal Patellofemoral Engagement (SPE) Index [21]. Radiographic classifications have been also reproduced with MRI [22]. Whilst patella height and engagement can be assessed in the sagittal plane, an appreciation of congruency especially through range of movement is not achieved.

280 Axial imaging provides information on the position of the patella within the
281 trochlear groove, however, static knee position images provide little information
282 toward the congruency or tracking through the range of movement. Skyline plain
283 radiographs have been found to be unreliable [23,24], because they can be difficult to
284 obtain at degrees of flexion less than 30 where subluxation is most prevalent. It is for
285 these reasons we sought to evaluate the patellofemoral joint by means of contact area
286 through axial MRI imaging during active movement as cartilage contact is the
287 functional basis of force transmission. Several other authors have previously given
288 attention to activation of the quadriceps mechanism during capture of axial imaging
289 [24-26].

290 Brossmann et al. used dynamic MRI to analyse patella tracking in healthy
291 volunteers and patients with maltracking [25]. They reported significantly different
292 patellar tracking patterns between the two groups and statistically significant tracking
293 differences between static and dynamic scanning of the PFJ although the contact
294 surface area was not a measured outcome. While McNally et al. described the
295 morphological traits of instability with dynamic axial MRI there was no recording of
296 congruency or contact area [26]. They demonstrated with the use of dynamic MRI that
297 patella subluxation was present in 40% of patients with anterior knee pain and
298 challenged the clinical relevance of mild subluxation of the PFJ. Martinez et al. utilised
299 CT scans at set intervals of 0, 20 and 45 degrees of flexion to establish the effect of
300 activation of the quadriceps on the centralisation and tilt of the patella [27]. The
301 individuals assessed had asymptomatic knees and were considered healthy. They
302 concluded that Quadriceps contraction had little influence on the patellar centralisation
303 and did not effect patellar tilt unless in full extension. The effect on unstable PFJs was
304 not explored by these authors.

We have sought to quantify the congruency of the PFJ through dynamic MRI mapping and 2D representation of contact surface area. We have documented the difference in contact surface area between the stable and unstable PFJ. The potential to use this MRI mapping methodology to establish the change in congruency for pre- and post-stabilisation surgeries will allow for objective evaluation of treatment modalities.

Despite the small sample size of this study there were significant differences in the contact area at all ranges between 0 and 40 degrees when comparing cases and controls. The gender imbalance of male n=7 to female n=2 in the control group is seen by the authors as a weakness of the study as the majority of PFJ instability cases are seen in the female population. The disadvantages of adding a dynamic element to MRI imaging has the potential for generation of movement artefact with the addition of a further variable which may increase the variance of the data. The issue of motion artefact was minimal as the rapid sequence MRI scan coupled with stabilisation of the femur resulted in clear and accurate images for interpretation. Despite the risk of motion artefact, the authors believe dynamic imaging of the PFJ may be more representative of the physiologic conditions that are present during ambulation. The range of movement is limited to 40 degrees of flexion due to the physical constraints of the MRI scanner.

The articulation of the PFJ, if accurately measured in terms of contact area, will provide useful information in determining the effectiveness of surgeries aimed at increasing congruency. The authors aim to compare a cohort of patients pre- and post-stabilisation surgery using this methodology to quantify the effects of surgical modalities on PFJ congruence.

Conclusion:

The unstable patellofemoral joint is less congruent than the stable patellofemoral joint throughout knee movement. The unstable PFJ has less contact surface area and this will inversely increase the contact pressure for a given force leading an increased risk of degeneration of the joint. This approach to mapping of the patellofemoral joint may aid in the design of operations to increase stability and serve to provide a means of assessing pre- and post-operative joint congruency as an outcome measure. If a single axial series is to be obtained on MRI scan, the authors recommend 10-20 degrees of tibiofemoral flexion as this was shown to have the greatest difference in contact surface area between the cases and controls group.

Figure 1: Flow chart of case inclusion and exclusion.

Figure 2: A: The subject lay supine on the MRI table with a triangular wedge under the knee. B: Foam blocks were placed for passive range of movement at 0, 20 and 40 degrees flexion. C: Deflating balloon against resistance with multiple sequence scans for Quadriceps active.

Figure 3: A beach ball was placed anterior to the tibia to provide resistance and achieve quadriceps activation. The subject controlled a valve to control the rate of deflation.

Figure 4: "Flattening" of axial imaging. Slices are at 5mm intervals. The width of each slice in which there is contact between femur and patella cartilage is multiplied by 5mm. Each measurement is then summed to give a total area of congruence.

Figure 5: Control vs Instability group in passive and active movement.

Figure 6: Histogram in quadriceps active, control and instability

Table 1: Age, Tibial Tuberosity Trochlear Groove (TTTG) distance (mm), Insall Salvati Ratio (ISR), Biedert Patellotrochlear Index, SD = standard deviation, n = number.

Table 2: Clinical comparison between cases and controls.

Table 3: Comparison of mean joint congruence between case and controls during quadriceps active knee movement.

REFERENCES:

1: Goodfellow J, Hungerford DS, Zindel M. Patello-femoral joint mechanics and pathology. 1. Functional anatomy of the patello-femoral joint. J Bone Joint Surg Br. 1976 Aug;58(3):287-90.

2: Dejour H, Walch G, Neyret P, Adelein P. Dysplasia of the femoral trochlea. Rev Chir Orthop 1990;76:45–54.

3: Eijkenboom JFA, Waarsing JH, Oei EHG, Bierma-Zeinstra SMA, van Middelkoop M. Is patellofemoral pain a precursor to osteoarthritis? Bone Joint Res. 2018 Oct 3;7(9):541-547.

4: Luyck T, Didden K, Vandenuecker H, Labey L, Innocenti B, Bellemans J. Is there a biomechanical explanation for anterior knee pain in patients with patella alta? J Bone Joint Surg Br 2009;91-B(3):344-350.

5: Conchie H, Clark D, Andrew M, Eldridge J, Whitehouse M. Adolescent knee pain and patellar dislocations are associated with patellofemoral osteoarthritis in adulthood: A case control study. Knee 2016;23(4):708-711.

6: Utting MR, Davies G, Newman JH. Is anterior knee pain a predisposing factor to patellofemoral osteoarthritis? Knee 2005;12(5):362–5.

388 7: Clark D, Metcalfe A, Wogan C, Mandalia V, Eldridge. Adolescent patellar
389 instability: current concepts review. J Bone Joint J. 2017 Feb;99-B(2):159-170.
390

391 8: Keller JM, Levine WN. Evaluation and Imaging of the Patellofemoral Joint.
392 Operative Techniques in Orthopaedics 2007;17(4):204-210.
393
394
395

396 9: Merchant AC, Mercer RL, Jacobsen RH, Cool CR. Roentgenographic analysis of
397 patellofemoral congruence. J Bone Joint Surg Am 1974;56:1391-1396 .
398

399 10: Oye CR, Holen KJ, Foss OA. Mapping of the femora trochlea in a newborn
400 population: an ultrasonographic study. Acta Radiol 2014;2:234-43.
401

402 11: Alemparte J, Ekdahl M, Burnier L, et al. Patellofemoral evaluation with
403 radiographs and computed tomography scans in 60 knees of asymptomatic subjects.
404 Arthroscopy 2007;23(2):170-177.
405

406 12: Wittstein JR, Bartlett EC, Easterbrook J, Byrd JC. Magnetic resonance imaging
407 evaluation of patellofemoral malalignment. Arthroscopy 2006;22:643-649.
408

409 11: Victor J, Van Glabbeek F, Vander Sloten J, Parizel PM, Somville J, Bellmans J. An
410 experimental model for kinematic analysis of the knee. J Bone Joint Surg Am
411 2009;91(6):150-63.
412

413 12: Hashimoto S, Ochs RL, Komiya S, Lotz M. Linkage of chondrocyte apoptosis and
414 cartilage degradation in human osteoarthritis. *Arthritis Rheum* 1998;41(9):1632-1638.
415

416 13: Saggin PR, Saggin JI, Dejour D. Imaging in patellofemoral instability: an
417 abnormality-based approach. *Sports Med Arthrosc* 2012;20(3):145-51.
418

419 14: Becker R, Hirschmann MT, Karlsson J. The complexity of patellofemoral
420 instability. *Knee Surg Sports Traumatol Arthrosc* 2018;26(3):675–676.
421

422 15: Senavongse W1, Farahmand F, Jones J, Andersen H, Bull AM, Amis AA.
423 Quantitative measurement of patellofemoral joint stability: force-displacement
424 behavior of the human patella in vitro. *J Orthop Res* 2003;21(5):780-6.
425

426 16: Staeubli HU, Bosshard C, Porcellini P, Rauschning W. Magnetic resonance
427 imaging for articular cartilage: cartilage-bone mismatch. *Clin Sports Med*
428 2002;21(3):417-33 [viii-ix].
429

430 17: Insall J, Salvati E. Patella position in the normal knee joint. *Radiology*
431 1971;101(1):101-104.
432

433 18: Grelsamer RP, Meadows S. The modified Insall-Salvati ratio for assessment of
434 patellar height. *Clin Orthop Relat Res* 1992;282:170-176.
435

436 19: Blackburne JS, Peel TE. A new method of measuring patellar height. *J Bone Joint*
437 *Surg Br* 1977;59(2):241-242.

438

439 20: Caton G, Deschamps, Chambat G, Lerat JL, Dejour H. Patella infera. Apropos of
440 128 cases. Rev Chir Orthop Reparatrice Appar Mot 1982;68(5):317-325.

441

442 21: Dejour D, Ferruaa P, Ntagiopoulos PG et al. The introduction of a new MRI index
443 to evaluate sagittal patellofemoral engagement. Orthop Traumatol Surg Res 2013;99(8
444 Suppl):S391-S398.

445

446 22: Miller TT, Staron RB, Feldman F. Patellar height on sagittal MR imaging of the
447 knee. Am J Roentgenol 1996;167(2):339-341.

448

449 23: Walker C, Cassar Pullicino VN, Vaisha R, McCall IW. The patello-femoral joint:
450 a critical appraisal of its geometric assessment utilizing conventional axial radiography
451 and computed arthro-tomography. Br J Radiol 1993;66(789):755-761.

452

453 24: Inoue M, Shino K, Hirose H, Horibe S, Ono K. Subluxation of the patella.
454 Computed tomography analysis of patellofemoral congruence. J Bone Joint Surg Am
455 1998;70(9):1331-1337.

456

457 25: Brossmann J, Muhle C, Schroder C et al. Patellar tracking patterns during active
458 and passive knee extension: evaluation with motion-triggered cine MR imaging.
459 Radiology 1993;187(1):205-212.

460

461 26: McNally EG, Ostlere SJ, Pal C, Phillips A, Reid H, Dodd C. Assessment of patellar
462 maltracking using combined static and dynamic MRI. Eur Radiol 2000;10(7):1051-5.

463

464 27: Martinez S, Korobkin M, Fondren FB, Hedlund, LW, Goldner JL. Computed

465 tomography of the normal patellofemoral joint. Invest Radiol 1983;18(3):249-53.

466

Figure 1: Flow chart of case inclusion and exclusion.

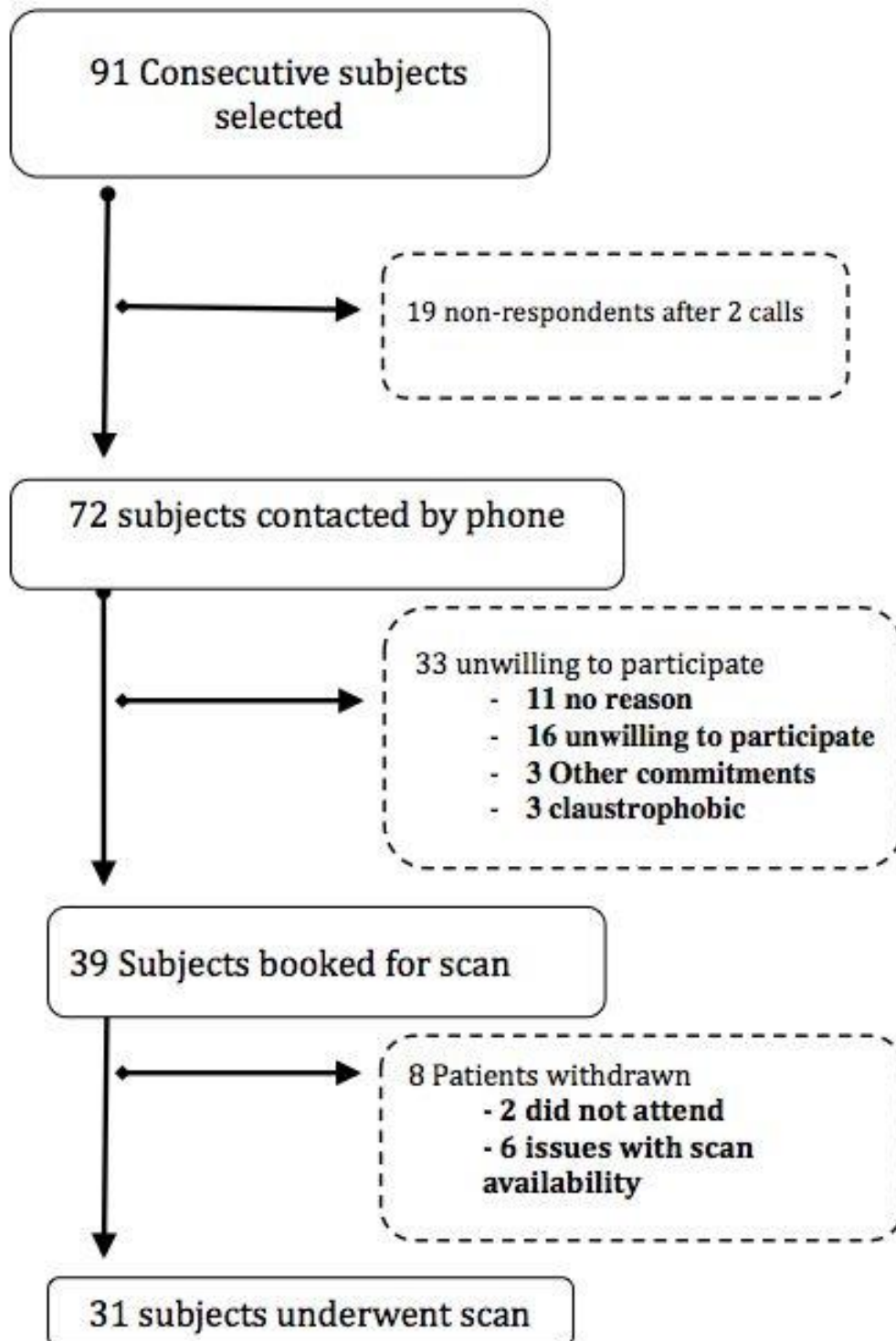


Figure 2: A: The subject lay supine on the MRI table with a triangular wedge under the knee. B: Foam blocks were placed for passive range of movement at 0, 20 and 40 degrees flexion. C: Deflating balloon against resistance with multiple sequence scans for Quadriceps active

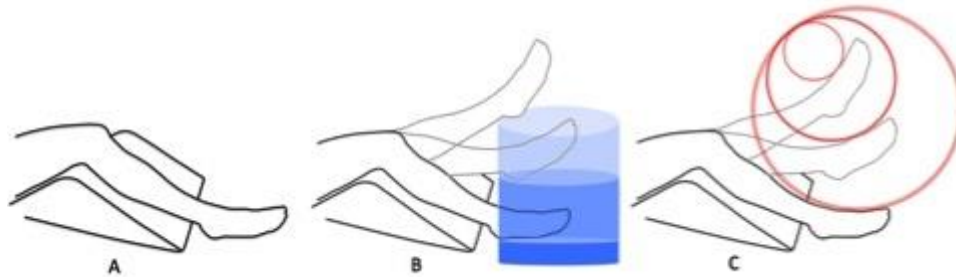


Figure 3: A beach ball was placed anterior to the tibia to provide resistance and achieve quadriceps activation. The subject controlled a valve to control the rate of deflation.

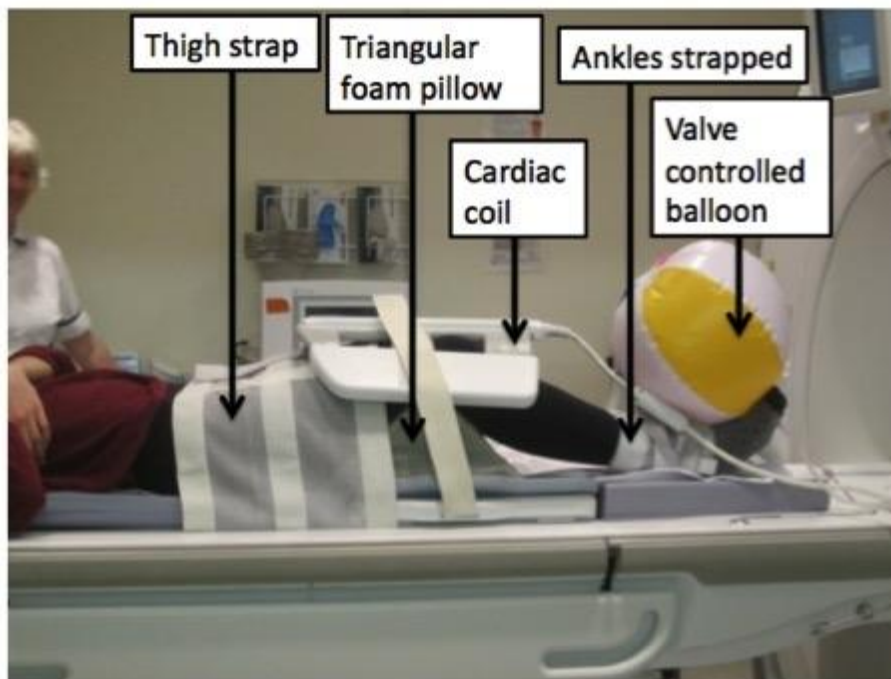
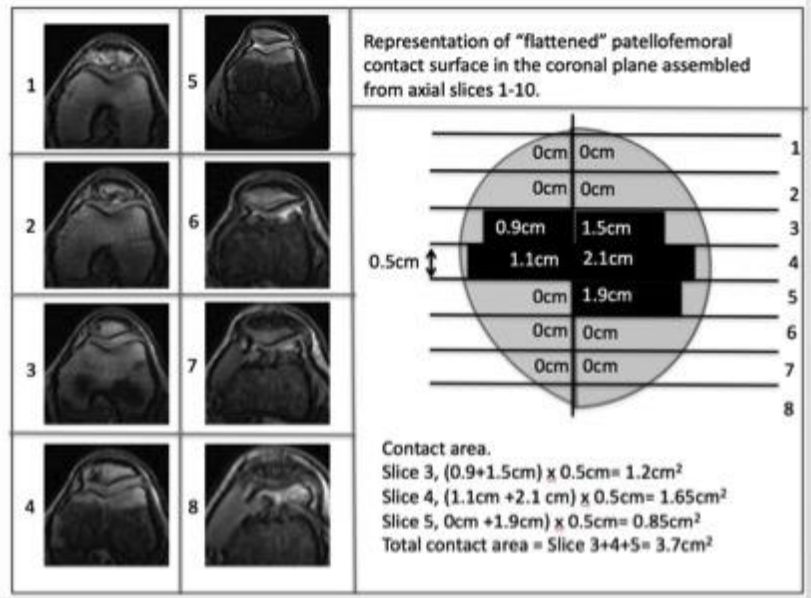
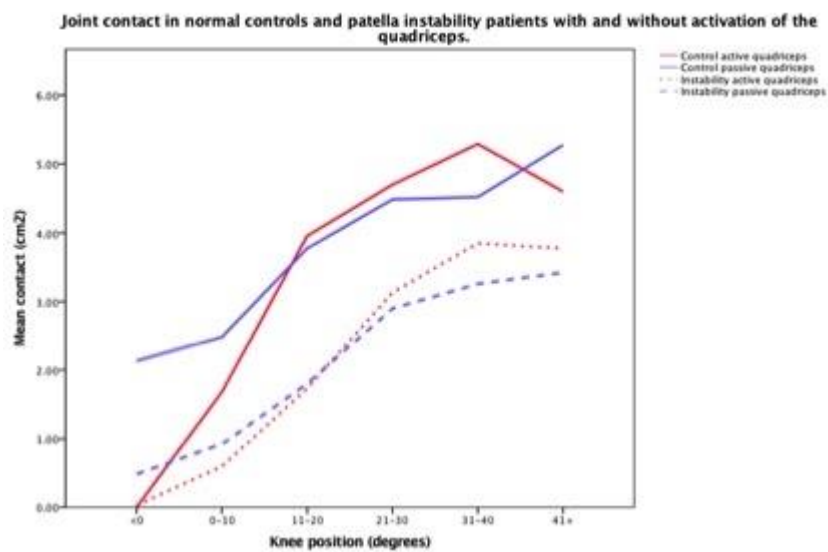


Figure 4: "Flattening" of axial imaging. Slices are at 5mm intervals. The width of each slice in which there is contact between femur and patella cartilage is multiplied by 5mm. Each measurement is then summed to give a total area of congruence.



490 **Figure 5:** Control vs Instability group in passive and active movement.

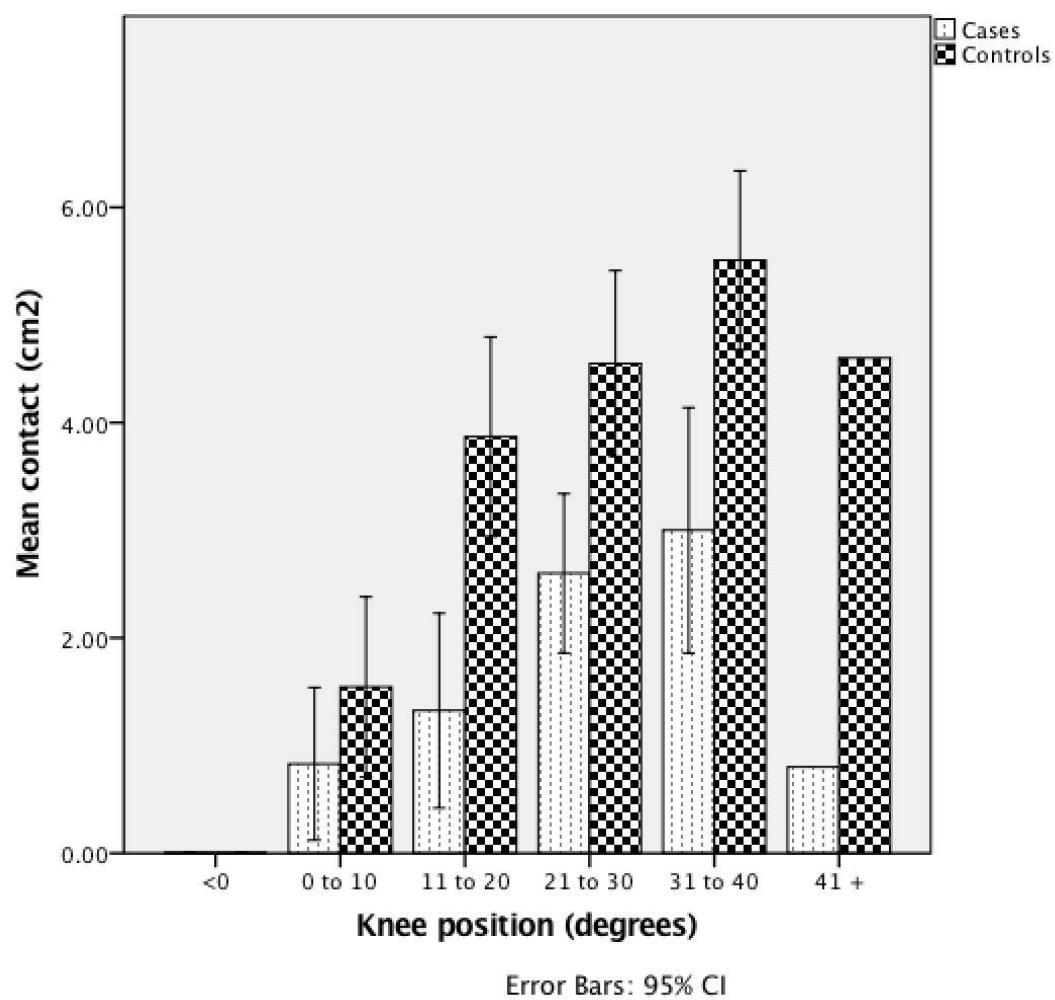


491

492

493

494 **Figure 6:** Histogram in quadriceps active, control and cases groups



495

496

497

	Cases			Controls			p value
	Mean	SD	n	Mean	SD	n	
Age	25	6.9	31	26	5.1	9	0.690
TTTG	13.3	4.6	31	11.9	3.2	9	0.400
ISR	1.37	0.2	31	1.19	0.09	9	0.013
Biedert	32.5	23	31	38.2	3.3	9	0.470
Age at 1st dislocation	14.9	3.8	21	-	-	-	

498

499 **Table 1:** Age, Tibial Tuberosity Trochlear Groove (TTTG) distance (mm), Insall

500 Salvati Ratio (ISR), Biedert Patellotrochlear Index, SD = standard deviation, n =

501 number

502

503

		Cases		Control		p value
		n	%	n	%	
Sex (female - male)		19 - 12	61 female	2-7	22.2 female	0.060
Laterality (left - right)		11 - 20	36 left	4-5	44 left	0.705
Dejour grade	Normal	6	19	9	100	0.001
	A	3	10	0	0	
	B	5	16	0	0	
	C	14	45	0	0	
	D	3	10	0	0	
Hypermobile (Beighton Score of 4+)		7/31	22.6	0/9	0	0.175
Previous surgery		7/31	22.6	0/9	0	0.175
Subjects with >2 dislocations		19/31	61	0/9	0	0.001

504

505

506

Table 2: Clinical comparison between cases and controls

507

Quadriceps active: knee position.		n	Mean joint congruence cm2	mean diff	95% lower	95% upper	P
<0	Case	7	0.029	0.029	-0.10	0.16	0.626
	Control	2	0.00				
0-10	Case	26	0.59	-1.09	-1.80	-0.38	0.004
	Control	11	1.68				
11-20	Case	26	1.73	-2.22	-3.16	-1.27	0.000
	Control	9	4.00				
21-30	Case	24	3.13	-1.57	-2.64	-0.49	0.006
	Control	8	4.70				
31-40	Case	18	3.85	-1.44	2.58	-0.30	0.016
	Control	5	5.29				
40+	Case	9	3.77	-0.83	-4.51	2.85	0.618
	Control	1	4.60				
Combined	Case	110	2.17	-1.24	-1.91	-0.55	0.000
	Control	36	3.40				

508

509 **Table 3:** Comparison of mean joint congruence between case and controls during

510 quadriceps active knee movement

511

512